Zeitschrift fr physikalische Chemie

Embedded cluster models for reactivity of the hydrated electron

M.Sc. Frank Uhlig: Institute of Organic Chemistry and Biochemistry, Academy of Sciences of the Czech Republic, Flemingovo nám, 2, CZ-16610 Prague, Czech Republic
Tel: +420-220-410314, Fax: +420-220-410320, E-Mail: frank.uhlig@uochb.cas.cz

Prof. Dr. Pavel Jungwirth: Institute of Organic Chemistry and Biochemistry, Academy of Sciences of the Czech Republic, Flemingovo nám, 2, CZ-16610 Prague, Czech Republic
Tel: +420-220-410314, Fax: +420-220-410320, E-Mail: pavel.jungwirth@uochb.cas.cz

Keywords: hydrated electron, reactivity, clusters, hydronium, nitrous oxide

Schlagworte: hydrated electron, reactivity, clusters, hydronium, nitrous oxide

MS-ID: Heft: / ()	pavel.jungwirth@uochb.cas.cz	April 19, 2013

Abstract

Our computational study presents embedded cluster models of the hydrated electron focusing on its reactivity with the hydrated proton and the nitrous oxide molecule leading to formation of a hydrogen atom in the former case and a nitrogen molecule plus hydroxyl radical and hydroxide anion in the latter case. We show using ab initio calculations combined with the nudged elastic band method for determining minimum energy paths that carefully chosen cluster models with no more than six water molecules embedded in a polarizable continuum are able to capture the essential features of the reactive processes of the hydrated electron.

1 Introduction

Solvated electron is a key intermediate in processes involving water radiolysis and photolysis [1]. Its lifetime in aqueous systems does not exceed milliseconds due to its high reactivity [2]. One of its most important reaction is that with a proton forming a hydrogen atom [1, 3, 4, 5, 6]. In the acidic aqueous nuclear waste this reaction can lead to formation of dangerous amounts of explosive hydrogen gas [1]. Therefore, chemicals which can quench the solvated electrons before hydrogen can be formed, need to be added. Among these, typical quenchers are N_2O, SF_6, and others [3, 7]. In order to devise efficient strategies how to compete with the electron-proton reaction, it is important to understand in detail its mechanism. Despite the seeming simplicity of this reaction the mechanism has been long debated [3, 4, 5]. It is now well established that the reaction is not diffusion limited, but about an order of magnitude slower [1, 8, 9]. This is due to the large rearrangements of the solvation shells of both H^+ and e^- when forming a neutral H atom [5, 10]. Moreover, the reaction is of a proton-transfer rather than electron-transfer character [4, 5]. This can be explained by the fact that the effective mass of a hydrated electron is larger than that of a proton in water [10], which can rapidly move via a hopping mechanism from one water molecule to another [11].

Quenching of solvated electrons takes place in liquid (or supercritical) water [7, 12], however, until recently most of the structural and energetic information about it has been obtained from cryogenic clusters [13]. Only in the last few years, photoelectron spectroscopy (PES) in aqueous microjets allowed to determine the vertical binding energy of an electron solvated in bulk liquid water, amounting to 3.3-3.6 eV [14, 15, 16, 17]. Calculations showed, that the most strongly bound isomers in large cryogenic clusters bear some resemblance to the ambient bulk hydrated electron, while the more weakly bound cluster isomers do not have an analogue in the liquid [18, 19]. Keeping this in mind we now critically examine the suitability of cluster models for investigating the reactivity of the solvated electron. An early picture of e^-_{aq} has been that of an excess negative charge surrounded octahedrally by six water molecules, which has been supported by electron spin echo measurements in concentrated alkaline glasses at low temperatures [20]. Hexacoordination of the solvated electron was also obtained from early pseudopotential calculations [21]. More recent pseudopotentials, as well as ab initio molecular dynamics (AIMD) point, however, to a roughly tetracoordinated e^-_{aq}, which is, incidentally, in accord with one of the oldest suggestions for the structure of the hydrated electron [22].

In our previous study, we showed that the electron-proton reaction in water can be successfully modelled using AIMD in a cluster system of 32 water molecules [10]. Subsequently, we demonstrated that the essential features of the reaction leading to formation of a hydrogen atom are preserved even in a smaller system with only four water molecules hy-

drating the proton and the electron [23], which was in accord with earlier calculations [24, 25, 26]. Here, we revisit this reaction focusing on "bulk-proxies" cluster structures with four and six water molecules embedded in a polarizable dielectric continuum. Additionally we address the reaction of the solvated electron with N_2O in embedded clusters with 5-6 water molecules, leading to the formation of a transient N_2O^- species [27, 28] which then further decomposes in water.

2 Methods

In the present study, geometry optimizations and minimum energy path (MEP) calculations in embedded cluster geometries were performed. As qualitative models for the reactivity of the bulk hydrated electron two clusters shown in Fig. 1 containing four or six water molecules plus an excess electron were considered. For the reaction of a proton and the hydrated electron a cluster containing six water molecules, a hydronium ion and an excess electron was employed as a starting point (see Fig. 2), since we have already explored the smaller system with four water molecules in our previous study [23]. To obtain a stable initial configuration for the reaction between nitrous oxide and the hydrated electron, several optimizations with varying numbers of additional water molecules solvating the N_2O were performed. Notably, no minimum structure with separated N_2O and e^-_{aq} could be obtained, since all optimizations yielded structures with the electron transfered to the nitrous oxide moiety and re-arranged water molecules in comparison to the starting $e^-(H_2O)_4$ or $e^-(H_2O)_6$ geometries.

The clusters were embedded in an implicit aqueous solvent by means of the conducter-like screening model (COSMO) as implemented in ORCA [29, 30]. For treatment of non-equilibrium processes of vertical ionization and optical absorption the non-equilibrium polarizable continuum model as implemented into GAUSSIAN 09 [31] was used.

MEPs were calculated with the nudged elastic band (NEB) method [32] with improved tangent estimates [33]. Initial guesses for the reaction path were obtained from linear interpolation between reactant and product structures. The NEB was first optimized without a climbing image, but the final reaction path calculations employ a climbing image to obtain the correct transition state structure [34]. For the individual optimizations of the NEBs the FIRE optimization procedure was used [35]. All geometry optimizations and MEP calcuations were done employing the Møller-Plesset perturbation theory of second order (MP2) for spin-polarized Hartree-Fock reference wavefunctions. Split-valence, atom-centered basis sets of double-ζ quality with polarization and diffuse functions on all atoms (6-31++G**) were used [36, 37]. The optimizations were performed with the atomistic simulation environment (ASE) [38]. Vertical detachment energies were calculated using the same setup as

Table 1: Vertical detachment energy (VDE) and first three excitation energies E_{exc} (in eV) of $e^-(H_2O)_4$ and $e^-(H_2O)_6$.

cluster	VDE [eV]	E_{exc} [eV]
$e^-(H_2O)_4$	2.920	1.546, 1.918, 1.921
$e^-(H_2O)_6$	3.244	1.683, 1.932, 1.932

above, but the structures were embedded into a non-equilibrium polarizable continuum model (NE-PCM) of the solvent. Similarly, excited states were obtained from clusters embedded in NE-PCM with time-dependent density functional theory (TD-DFT) with the 6-31++G** basis set and the Becke-Lee-Yang-Parr exchange-correlation functional [39, 40].

3 Results and Discussion

3.1 Embedded cluster models for e^-_{aq}

Stable minimum structures, similar to clusters previously proposed in the literature [22, 20], were investigated with respect to their capability of representing the bulk features of the hydrated electron. Two of the most important observables characterizing the hydrated electron are its vertical detachment energy (VDE) and the optical absorption spectrum. VDEs and the first three excitation energies for $e^-(H_2O)_4$ and $e^-(H_2O)_6$ clusters embedded in a polarizable continuum model of the solvent in geometries depicted in Figure 1 are summarized in Table 1. The vertical detachment energies are 2.9 eV and 3.2 eV for $e^-(H_2O)_4$ and $e^-(H_2O)_6$, respectively, which is close to the experimentally determined VDEs from different photoelectron spectroscopy studies on liquid microjet ranging from 3.3 to 3.6 eV [14, 15, 16, 17]. The optical spectrum of the hydrated electron is constituted by three s→p-like transitions lying around 1.7 eV and a slowly decaying blue tail [41]. The latter originates from a number of higher lying excited states and involves a comparably large electronic contribution of the solvent. The blue tail is not reproducible by either of the embedded cluster models as the systems are too small; nevertheless, the first three excitation energies (Table 1) are close to the observed experimental results. The microsolvation approach combined with the non-equilibrium continuum solvation model was shown to provide good agreement with experimental data for ionic solutes in the aqueous bulk previously. [42]. Both embedded cluster models thus show an acceptable agreement with experimental spectrum. The $e^-(H_2O)_6$ structure shows slightly higher ionization and excitation energies than the cluster with four water molecules.

From these points of view both embedded cluster models provide a reasonable comparison to the experimentally available data. To further

Table 2: Dissection of spin density into contributions from cavity, overlap with water molecules and diffuse, interstitial parts (in percent of total integrated spin).

	$e^-(H_2O)_4$	$e^-(H_2O)_6$
cavity	54.11 %	49.96 %
on water	9.10 %	11.03 %
diffuse	36.79 %	39.01 %

assess the validity of either of the models we make comparison to recent ab initio molecular dynamics (AIMD) simulations of a bulk hydrated electron [43]. The unpaired spin density corresponding to the hydrated electron can be divided into contributions from an inner cavity, overlap with neighboring water molecules, and a diffuse, interstitial part [43]. Again, both embedded cluster models show comparable results. The cavity contribution constitutes roughly 50 % of the hydrated electron, being about 5 % larger in the smaller cluster than in the larger one (Table 2). Overlap with water molecules accounts for about 10 % and the residual diffuse part is between 37 and 39 % of the total density. This is in a semi-quantitative agreement with the bulk result [43]. Nevertheless, the hydrated electron is diffuse in nature and spreads also over the second solvent shell, which is not included in the embedded cluster models. This explains the somewhat different partitioning values compared to the bulk solvated electron. The closer match between the bulk simulations and the larger cluster results is likely due to the two additional explicit water molecules that recover some of the second solvent shell contribution.

From a structural point of view, the $e^-(H_2O)_4$ cluster provides, however, a more consistent match than $e^-(H_2O)_6$, when compared to the ab initio simulations, as well as to most of the one-electron pseudopotentials in the aqueous bulk. The coordination number of water molecules in the first solvent shell as calculated with the above methodologies is typically about four [43, 44, 45]. The first peak of the radial distribution of oxygen atoms around the center of the spin density from the AIMD simulations is located at 2.5 Å, while the corresponding distance of the oxygen atoms of all water molecules is 2.8 Å for $e^-(H_2O)_4$ and 3.0 Å for $e^-(H_2O)_6$. This comparison thus again points to the former as the more appropriate choice of an embedded cluster model for the reactivity of the bulk hydrated electron.

3.2 Electron-proton reaction

A stable minimum structure of the hydrated electron and a hydronium ion in the embedded four-water-molecule cluster was only observed if the H_3O^+ moiety was first solvated by at least two water molecules that themselves are coordinated to the solvent cage of the hydrated electron.

In contrast, structures where a bare H_3O^+ ion was added to the embedded cluster model showed immediate proton transfer to one of the water molecules directly surrounding the hydrated electron. If H_3O^+ was added to the embedded water anion cluster with six H_2O molecules surrounding the excess electron, structures rearrange during optimization from two different initial conditions to a four-fold coordinated excess electron with H_3O^+ either directly being part of the excess electron solvation cage or coordinated to the latter and bridged by additional water molecules. These structures were higher in energy than the stable reaction cluster presented in Figure 3 and do not represent stable minimal geometries. Hence, no reaction paths were calculated for them. The reaction path obtained from the NEB calculations of our model system $e^-(H_2O)_6H_3O^+$, created by adding a di-hydrated hydronium to a tetra-hydrated electron, is shown in Figure 3.

The reaction in both systems, i.e., $e^-(H_2O)_3H_3O^+$ and $e^-(H_2O)_6H_3O^+$, proceeds via an initial compression of the solvent cage of the hydrated electron followed by a concerted proton transfer to one of the water molecules solvating the excess electron and, consequently, from that respective water molecule toward the center of the spin distribution. The effect of the embedding on the reaction cannot be directly quantified by recalculating the reaction path without COSMO since the reactant models are stable minima only when embedded into the polarizable continuum. Compared to previous investigations of a smaller and isolated reaction model $e^-(H_2O)_3H_3O^+$ [24, 23], the present reaction is less exoergic due to a better hydration of the two charged reactants in a larger water cluster embedded, moreover, in a dielectric continuum. Continuum solvation effects on the reaction barrier are, in contrast, very small, the small cluster model thus yielding correct kinetic description.

3.3 Nitrous oxide reaction

The net reaction of the nitrous oxide molecule with the hydrated electron reads as follows:

$$N_2O_{aq} + e^-_{aq} \longrightarrow N_2 + OH^{\bullet}_{aq} + OH^-_{aq}$$

The reaction proceeds via an intermediate oxygen anion solvated by water that in turn forms a hydroxyl radical and hydroxide anion by proton transfer from the surrounding water molecules.

As mentioned in the Methods section, no stable minimum structure could be obtained of a cluster containing a separated nitrous oxide molecule and a hydrated electron. Several clusters of different sizes and solvation structures of the nitrous oxide were investigated. All showed an immediate transfer of the excess electron to the N_2O moiety and a consequent rearrangement of water forming hydrogen bonds toward the oxygen atom of N_2O^-. After this rearrangement already 75 % of the excess charge is located on the N_2O moiety.

In Figure 4 the minimum energy path for transfer of the oxygen anion of N_2O^- to the surrounding water molecules is shown. The reaction has a small barrier of only 0.1 eV and the length of the path from initial minimum structure to transition state is relatively short. In the initial stage rotation of the bent N_2O^- around the cluster is observed, which is not associated with any large change in energy. The reaction then proceeds via a small barrier solely associated with the dissociation of the NO bond. This is exemplified in Figure 4 presenting the evolution of length of the NO bond, together with distances of hydrogen atoms close to the nitrous oxide oxygen atom. Further stabilization of the nascent structure is achieved by reorientation of surrounding water molecules pointing towards the O^- anion.

From this intermediate product the reaction proceeds via proton transfer from surrounding water molecules leading to formation of a hydroxyl radical and hydroxide anion. This reaction is known to proceed very fast and in experiments O^- only plays a significant role in highly basis solution starting from pH=12 [46]. Interestingly, within the cluster geometry shown in Figure 4 no structure with a hydroxyl radical could be obtained that had a lower energy than the solvated oxgyen anion.

4 Conclusion

In this study, we first examined two structures that are commonly associated with the hydrated electron. They consist of an electron solvated by either four or six water molecules and both have been invoked as structural motif of the hydrated electron in bulk solution. The four-fold coordination appears consistently throughout latest pseudopotential literature and ab initio molecular dynamics [44, 45]. Additionally, we invoked a six-coordinated model, which was deduced from measurements in cold, alkaline glasses [20]. Both four-and six fold coordinated embedded cluster models are capable of reproducing experimental observables reasonably well.

In the next step, we employed the embedded cluster models for investigating the reactivity of the hydrated electron. One caveat of cluster investigations of the proton-electron reaction is that bulk solvent effects are not fully accounted for and the solvent structure around the excess electron is not necessarily the same as in bulk solution. Structures that contain only about half of the solvent shell around the excess electron are observed if only small clusters are taken into account. This can be remedied by investigating larger clusters, nevertheless the overall reaction mechanism stays the same [10]. By implicitly accounting for solvent effects and considering a full solvation cage in this study, the reaction barrier increases by about 0.1 eV, with the overall mechanism remaining qualitatively the same.

For the reaction of the hydrated electron with the nitrous oxide molecule,

up to now only N_2O^- embedded in a polarizable continuum model (PCM) has been considered [27, 28]. Two structures differing in their respective NNO angle (132° and 180°) were investigated, with the collinear one yielding a slightly lower reaction barrier. In the clusters that we initially investigated only bent structures were observed that represented a true minimum on the potential energy surface. The minimum energy path in the present embedded cluster has an energy barrier reduced by more than a factor of two compared to that of a bare N_2O^- in PCM. Little structural change is needed to dissociate N_2O^-. The reaction between N_2O and the hydrated electron is not diffusion limited [47], indicating that a barrier has to be overcome to form the N_2O^- anion. Considering the instability of separated N_2O and hydrated electron in our small clusters, this barrier may though be very small.

In summary, we have examined the applicability of embedded cluster models for computational investigations of the reactivity of the hydrated electron showing that they can capture semiquantitatively the reaction mechanisms.

5 Acknowledgement

Support Czech Science Foundation (grant P208/12/G016) and the Academy of Sciences (Praemium Academie award) is gratefully acknowledged. FU acknowledges support from the IMPRS Dresden.

References

[1] B. C. Garrett et al., Chem. Rev **105** (2005) 355–389.

[2] K. Yokoyama, C. Silva, D. H. Son, P. K. Walhout, P. F. Barbara, J. Phys. Chem. A **102** (1998) 6957–6966.

[3] E. Hart, M. Anbar, The hydrated electron, Wiley-Interscience: New York (1970).

[4] G. Stein, Isr. J. Chem. **9** (1971) 413–418.

[5] P. Han, D. M. Bartels, J. Phys. Chem. **96** (1992) 4899–4906.

[6] H. Shiraishi, G. R. Sunaryo, K. Ishigure, J. Phys. Chem. **98** (1994) 5164–5173.

[7] P. M. Hare, E. A. Price, C. M. Stanisky, I. Janik, D. M. Bartels, J. Phys. Chem. A **114** (2010) 1766–1775.

[8] G. C. Barker, P. Fowles, D. C. Sammon, B. Stringer, Trans. Faraday Soc. **66** (1970) 1498–1508.

[9] J. A. Kloepfer, V. H. Vilchiz, V. A. Lenchenkov, X. Y. Chen, S. E. Bradforth, J. Chem. Phys. **117** (2002) 766–778.

[10] O. Marsalek, T. Frigato, J. VandeVondele, S. E. Bradforth, B. Schmidt, C. Schütte, P. Jungwirth, J. Phys. Chem. B **114** (2010) 915–920

[11] N. Agmon, Chem. Phys. Lett. **244** (1995) 456–462.

[12] D. M. Bartels, K. Takahashi, J. A. Cline, T. W. Marin, C. D. Jonah, J. Phys. Chem. A **109** (2005) 1299–1307.

[13] R. M. Young, D. M. Neumark, Chem. Rev. **112** (2012) 5553–5577.

[14] K. R. Siefermann, Y. Liu, E. Lugovoy, O. Link, M. Faubel, U. Buck, B. Winter, B. Abel, Nature Chem. **2** (2010) 274–279.

[15] A. T. Shreve, T. A. Yen, D. M. Neumark, Chem. Phys. Lett. **493** (2010) 216–219.

[16] Y. Tang, H. Shen, K. Sekiguchi, N. Kurahashi, T. Mizuno, Y. Suzuki, T. Suzuki, Phys. Chem. Chem. Phys. **12** (2010) 3653–5.

[17] F. Buchner, T. Schultz, A. Luebcke, Phys. Chem. Chem. Phys. **14** (2012) 5837–5842.

[18] A. Madarasz, P. J. Rossky, L. Turi, J. Chem. Phys. **130** (2009) 124319.

[19] O. Marsalek, F. Uhlig, T. Frigato, B. Schmidt, P. Jungwirth, Phys. Rev. Lett. **105** (2010) 043002.

[20] P. Narayana, M. Bowman, L. Kevan, V. Yudanov, Y. Tsvetkov, J. Chem. Phys. **63** (1975) 3365–3371.

[21] J. Schnitker, P. Rossky, J. Chem. Phys. **86** (1987) 3471–3485.

[22] M. Natori, T. Watanabe, J. Phys. Soc. Jpn. **21** (1966) 1573–1578.

[23] F. Uhlig, O. Marsalek, P. Jungwirth, Phys. Chem. Chem. Phys. **13** (2011) 14003–14009.

[24] A. L. Sobolewski, W. Domcke, Phys. Chem. Chem. Phys. **4** (2002) 4–10.

[25] A. L. Sobolewski, W. Domcke, Phys. Chem. Chem. Phys. **9** (2007) 3818–29.

[26] M. Oncak, P. Slavicek, M. Farnik, U. Buck, J. Phys. Chem. A **115** (2011) 6155–6168.

[27] E. Kryachko, C. Vinckier, M. Nguyen, J. Chem. Phys. **114** (2001) 7911–7917.

[28] K. Takahashi, S. Ohgami, Y. Koyama, S. Sawamura, T. Marin, D. Bartels, C. Jonah, Chem. Phys. Lett. **383** (2004) 445–450.

[29] S. Sinnecker, A. Rajendran, A. Klamt, M. Diedenhofen, F. Neese, J. Phys. Chem. A **110** (2006) 2235–2245.

[30] F. Neese, Wiley Interdiscip. Rev. Comput. Mol. Sci. **2** (2012) 73–78.

[31] M. J. Frisch et al., Gaussian 09 Revision A.1, Gaussian Inc. Wallingford CT (2009).

[32] H. Jonsson, G. Mills, K. W. Jacobson, Classical and Quantum Dynamics in Condensed Phase Simulations, World Scientific (1998).

[33] G. Henkelman, H. Jonsson, J. Chem. Phys. **113** (2000) 9978–9985.

[34] G. Henkelman, B. Uberuaga, H. Jonsson, J. Chem. Phys. **113** (2000) 9901–9904.

[35] E. Bitzek, P. Koskinen, F. Gähler, M. Moseler, P. Gumbsch, Phys. Rev. Lett. **97** (2006) 170201.

[36] W. Hehre, R. Ditchfield, J. Pople, J. Chem. Phys. **56** (1972) 2257–2261.

[37] R. Krishnan, J. Binkley, R. Seeger, J. Pople, J. Chem. Phys. **72** (1980) 650–654.

[38] S. R. Bahn, K. W. Jacobsen, Comput. Sci. Eng. **4** (2002) 56–66.

[39] A. Becke, Phys. Rev. A **38** (1988) 3098–3100.

[40] C. Lee, W. Yang, R. Parr, Phys. Rev. B **37** (1988) 785–789.

[41] J. M. Herbert, L. D. Jacobson, J. Phys. Chem. A **115** (2011) 14470–14483.

[42] E. Pluharova, P. Jungwirth, S. E. Bradforth, P. Slavicek, J. Phys. Chem. B **115** (2011) 1294–1305.

[43] F. Uhlig, O. Marsalek, P. Jungwirth, J. Phys. Chem. Lett. **3** (2012) 3071–3075.

[44] L. Turi, D. Borgis, J. Chem. Phys. **117** (2002) 6186–6195.

[45] L. D. Jacobson, J. M. Herbert, J. Chem. Phys. **133** (2010) 154506.

[46] G. V. Buxton, C. L. Greenstock, W. P. Helman, A. B. Ross, J. Phys. Chem. Ref. Data **17** (1988) 513–886.

[47] K. Takahashi, D. M. Bartels, J. A. Cline, C. D. Jonah, Chem. Phys. Lett. **357** (2002) 358–364.

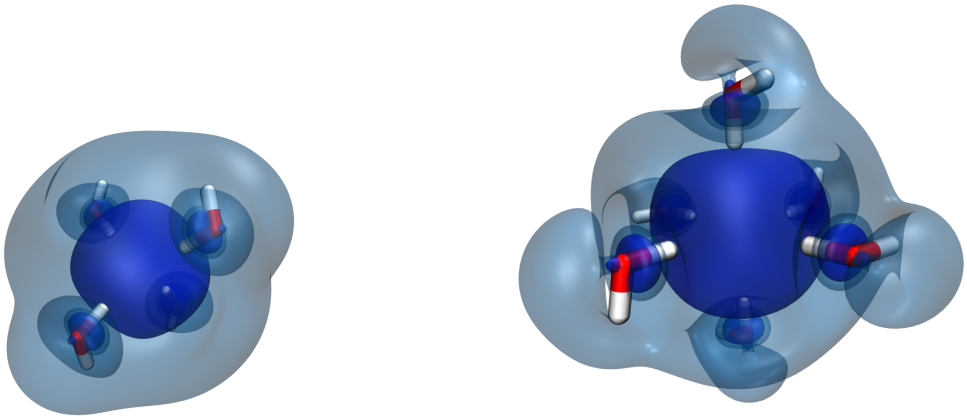

$e^-(H_2O)_4$ $e^-(H_2O)_6$

Figure 1: Minimal cluster models of the hydrated electron; either four (left) or six (right) water molecules plus an excess electron embedded in conductor-like solvent environment

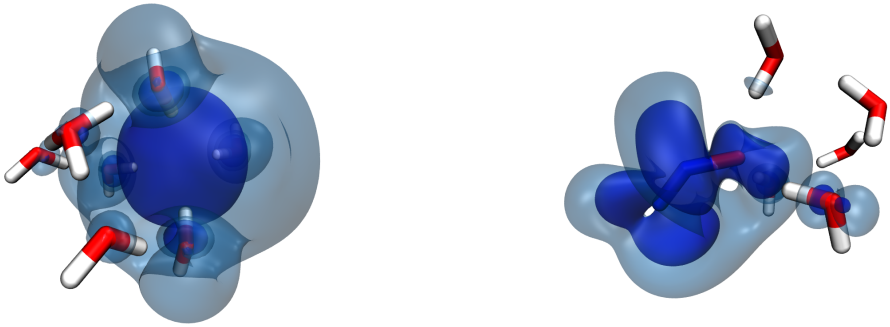

$e^-(H_2O)_6H_3O^+$ $(H_2O)_5N_2O^-$

Figure 2: Clusters embedded in conducter-like solvent environment considered for the reaction of a hydrated electron and a proton (left) and the reaction of N_2O with a hydrated electron (right).

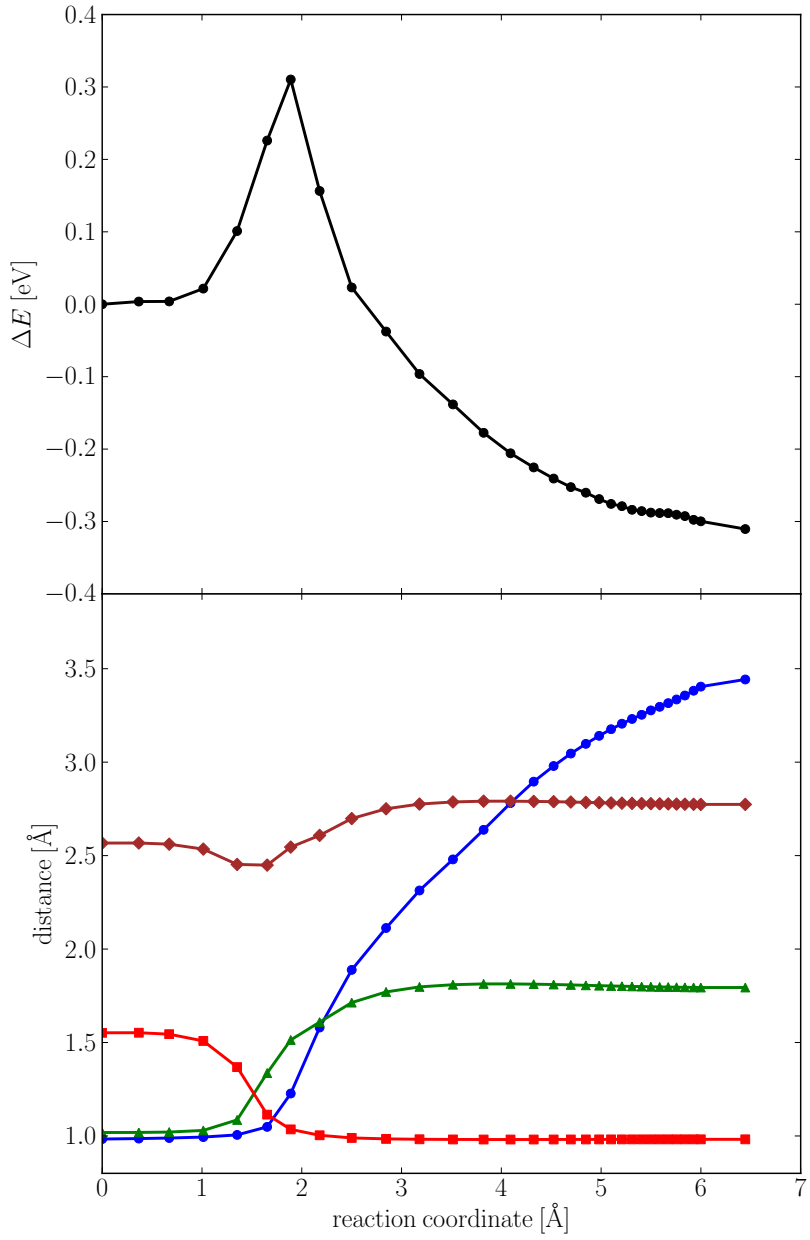

Figure 3: Top: MEP for the reaction of the hydrated proton with the hydrated electron in the embedded cluster model $e^-(H_2O)_6H_3O^+$. Bond distances along reaction paths in $e^-(H_2O)_6H_3O^+$; OH bond in H_3O^+ (triangles), distance of proton in H_3O^+ to oxygen atom of the H_2O the proton is transfered to (squares), OH distance in H_2O that delivers reactive proton (circles), and distance of oxygen atoms between H_3O^+ and H_2O molecule (diamonds). The seeming cusp in the upper plot is due to the finite number of images used in the nudged elastic band calculation.

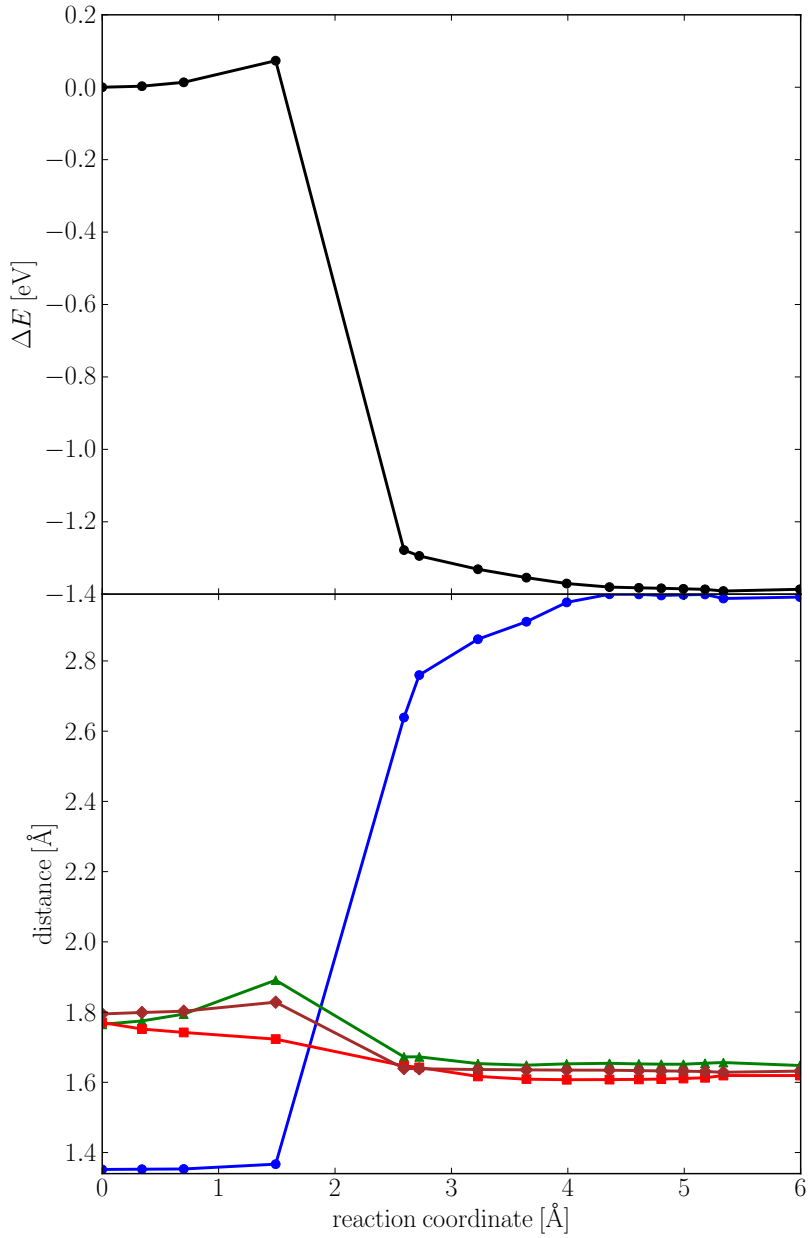

Figure 4: Top: MEP for the reaction of nitrous oxide anion solvated by five water molecules. Bottom: Length of the NO bond (circles) and distances of hydrogen atoms in water molecules surrounding N_2O^- to the nascent oxygen anion (diamonds, circles, and squares).